

Article

Effect of Modified Tetraethyl Orthosilicate Surface Treatment Agents on the Permeability of Airport Pavement Concrete

Tianlun Li  and Yonggen Wu *

Aviation Engineering School, Air Force Engineering University, Xi'an 710038, China; litianlun2020@163.com

* Correspondence: wuyonggen1@163.com

Abstract: In this paper, three modified tetraethyl orthosilicate surface treatment agents were prepared by using tetraethyl orthosilicate (TEOS) as the preparation monomer, isobutyltriethoxysilane (IBTS) as the hybridizer, and acrylic acid, phosphoric acid, and hydrochloric acid as the catalysts. The effects of the three modified tetraethyl orthosilicate surface treatment agents on the permeability of airport pavement surface concrete were investigated by water absorption tests, water contact angle tests, water penetration resistance tests, chloride ion penetration resistance tests, and carbonation tests, and the mechanisms of action of the modified tetraethyl orthosilicate surface treatment agents were analyzed by microscopic tests. The results showed that all three tetraethyl orthosilicate surface treatment agents could significantly improve the impermeability of concrete, among which the modified tetraethyl orthosilicate surface treatment agent with hydrochloric acid as the catalyst had the most obvious effect on the improvement of the impermeability of concrete. Acrylic acid was weaker than hydrochloric acid as the catalyst of a modified tetraethyl orthosilicate surface treatment agent for the improvement of concrete impermeability; it was only slightly stronger than hydrochloric acid as the catalyst of modified tetraethyl orthosilicate surface treatment agent in terms of the improvement of concrete's resistance to water penetration, and the difference between the two was not significant. Phosphoric acid as a catalyst of the modified tetraethyl orthosilicate surface treatment agent was the least effective for concrete impermeability; it was only stronger than the other two modified tetraethyl orthosilicate surface treatment agents in the improvement of concrete resistance to carbonation, and the carbonation depth of the concrete was only 1 mm in 28 days. SEM and MIP tests showed that the modified tetraethyl orthosilicate surface treatment agents improved the impermeability of concrete mainly by producing additional hydrated calcium silicate gel to plug microcracks and pores, reduce the total porosity of the concrete and the number of multi-harmful and harmful pores, and improve the compactness of the concrete. The test results can provide a reference for the development of modified tetraethyl orthosilicate surface treatment agents and their application in airport pavement surface engineering.

Keywords: concrete; surface treatment; tetraethyl orthosilicate (TEOS); hybridizer; catalyst; permeability



Citation: Li, T.; Wu, Y. Effect of Modified Tetraethyl Orthosilicate Surface Treatment Agents on the Permeability of Airport Pavement Concrete. *Coatings* **2022**, *12*, 1027. <https://doi.org/10.3390/coatings12071027>

Academic Editor: Waseem Haider

Received: 22 June 2022

Accepted: 18 July 2022

Published: 20 July 2022

Publisher's Note: MDPI stays neutral with regard to jurisdictional claims in published maps and institutional affiliations.



Copyright: © 2022 by the authors. Licensee MDPI, Basel, Switzerland. This article is an open access article distributed under the terms and conditions of the Creative Commons Attribution (CC BY) license (<https://creativecommons.org/licenses/by/4.0/>).

1. Introduction

During the service process, the cement concrete pavement of airports is subject to multiple factors, such as aircraft loading, freeze–thaw cycles, chloride ion penetration, carbonation, sulfate erosion, and alkali–aggregate reaction [1–3]. In recent years, many airports have experienced cracks, spalling, warping, misalignment, and even sand and stones in the process of cement concrete pavement [4,5], which mainly reflects the durability of concrete, seriously affects the normal operation of airport runways and the safety of aircraft takeoff and landing, and may even cause the failure of runway function or serious flight accidents [6,7]. In addition, the combination of a harsh climatic environment, frequent sudden natural disasters, and an unnatural environment (such as de-icing salt) accelerates the damage and service-life shortening of airport concrete pavement surfaces [8–10]. Concrete's carbonation, water and chloride ion penetration, sulfate corrosion, freeze–thaw

damage, and alkali–aggregate reaction are all related to its permeability [11]. There is a close correlation between concrete permeability and durability, and Mehta et al. [12] found that “in the long run, the permeability or water penetration of concrete is the only feature directly related to durability”. The permeability of concrete largely determines its durability.

Surface treatment is an economically feasible, simple, and effective method that can effectively improve the permeability of concrete [13–17]. In recent years, tetraethyl orthosilicate has been increasingly used for the surface treatment of cementitious materials, and good results have been achieved. Pigino et al. [18] found that tetraethyl orthosilicate was able to penetrate concrete to a depth of about 3–5 mm, and resulted in significant decreases in water absorption, chloride diffusion coefficient, and carbonation depth. Franzoni et al. [19] studied and compared the effectiveness of tetraethyl orthosilicate, sodium silicate solution, and nanosilica on the surface treatment of reinforced concrete structures in terms of morphology and microstructure, and showed that tetraethyl orthosilicate performed the best in terms of resistance to water penetration, chloride penetration, and carbonation, with significant improvements. García-Vera et al. [20] found that tetraethyl orthosilicate can reduce the total volume of pores in stucco, reduce the capillary water absorption and permeability of stucco, and reduce the impact of rain, acid rain, and sulfuric acid on stucco’s durability. Franzoni et al. [21] investigated the effects of TEOS treatment by piezometric porosimetry, scanning electron microscopy, water absorption, compressive strength tests, and spectrophotometry, and the results showed that the TEOS-treated sintered clay brick samples had a good penetration depth (about 10 mm), a reduction in porosity, a significant reduction in water absorption, a significant increase in compressive strength, and a positive aesthetic effect. Cai et al. [22] investigated the effects of surface treatment of hardened cementitious materials with tetraethyl orthosilicate, and showed that tetraethyl orthosilicate significantly reduced the water absorption rate and water vapor transport properties of the materials. Barberena-Fernández et al. [23] investigated the effects of tetraethyl orthosilicate as a surface curing agent for cement mortars, and the results showed that tetraethyl orthosilicate could improve the strength of cement mortars, reduce their porosity and permeability, and minimize the degree of alteration in their appearance. Microscopic tests showed that tetraethyl orthosilicate interacts with C-S-H gel—a product of cement hydration—and can form a longer gel chain than cement. Chen et al. [24] synthesized a composite emulsion of tetraethyl orthosilicate and isobutyltriethoxysilane, and demonstrated that this composite emulsion, when applied to concrete, could improve the waterproofing effect, gas penetration resistance, and surface strength of concrete, helping to further improve the durability of the concrete.

However, tetraethyl orthosilicate has some drawbacks when applied as a surface treatment, mainly in the form of slow curing reaction [25,26], cracking during drying and shrinkage [18], etc. Existing studies have shown that the addition of some nanoparticles [26,27], catalysts, or silane/siloxane hybridization [28–30] can overcome these drawbacks to some extent. Chen et al. [31] prepared a permeable waterproof material by sol–gel synthesis of TEOS and isobutylsilane, and studied its effects on the concrete surface. The results showed that the conforming emulsion could reduce the capillary absorption coefficient by more than 80%, and could also improve the carbonation resistance of concrete. Ramón Zárraga et al. [32] found that the addition of polydimethylsiloxane (PDMS) as a hybridizer to dibutyltin dilaurate (DBTL)-catalyzed TEOS-based curing agents could be achieved through the generation of rigid three-dimensional SiO₂ gel tautomerization to reduce cracking problems during stone curing, and that the ability of the curing agent to penetrate the porous structure of the stone remained almost unchanged with the addition of PDMS, and also reduced the percentage of volatile organic components and improved resistance to water penetration. However, there has been no systematic study on the modification of tetraethyl orthosilicate for application on concrete pavements.

Therefore, in this study, a modified tetraethyl orthosilicate surface treatment agent was prepared using tetraethyl orthosilicate as the preparative monomer, isobutyltriethoxysilane

as the hybridizing agent, and acrylic acid, phosphoric acid, and hydrochloric acid as catalysts. The effects of the modified tetraethyl orthosilicate surface treatment agent on the impermeability of the airport pavement surface concrete were studied through water absorption tests, hydrophobicity tests, water penetration resistance tests, chloride ion penetration resistance tests, and carbonation tests, and its mechanism of action was investigated by microscopic tests. It is hoped that our results can provide a reference for the development of modified tetraethyl orthosilicate surface treatment agents and their application in airport pavement surface projects.

2. Experimental Section

2.1. Materials

2.1.1. Concrete

The cement was 42.5 ordinary silicate cement, with a density and specific surface area of 3.15 g/cm^3 and $346 \text{ m}^2/\text{kg}$, respectively. The fine aggregate was washed Bahe River sand from Shaanxi Province, Xi'an, China, with a fineness modulus of 2.75 and apparent density of 2.72 g/cm^3 . The coarse aggregate was crushed limestone, with particle sizes in the ranges 5–10, 10–20, and 20–40 mm at a mixing ratio of 1:2:3. The water was ordinary tap water, and the water-reducing agent was FDN-C naphthalene water-reducing agent.

According to the results of the preliminary laboratory testing, the concrete ratio and performance index used in this paper are shown in Table 1.

Table 1. Mix proportion and properties of concrete.

Cement (kg/m^3)	Fine Aggregate (kg/m^3)	Coarse Aggregate (kg/m^3)	Water (kg/m^3)	Water- Reducing Agent	Water Cement Ratio	Vebe Consistometer/s	Flexural Strength at 28 d/MPa
330	630	1328	135.3	0.2%	0.41	22	5.6

2.1.2. Modified Tetraethyl Orthosilicate Surface Treatment Agent

Tetraethyl orthosilicate, isobutyltriethoxysilane, acrylic acid, hydrochloric acid, phosphoric acid, anhydrous ethanol, wetting agents, and distilled water were used in the experiments. The molecular formula of tetraethyl orthosilicate is $\text{C}_8\text{H}_{20}\text{O}_4\text{Si}$, and its molecular structure is shown in Figure 1a. The molecular formula of isobutyltriethoxysilane is $\text{C}_{10}\text{H}_{24}\text{O}_3\text{Si}$, and its molecular structure is shown in Figure 1b.

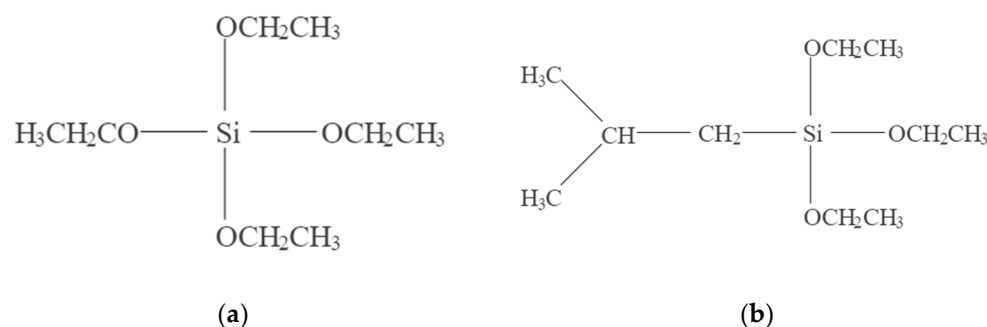


Figure 1. Molecular structure of (a) tetraethyl orthosilicate and (b) isobutyltriethoxysilane.

The preparation process of the modified tetraethyl orthosilicate surface treatment agent is as follows: First, stir anhydrous ethanol and distilled water in a high-speed dispersant to warm up, and then slowly drop in the acid catalyst (acrylic acid, phosphoric acid, or hydrochloric acid) to adjust the pH value. Next, slowly add the mixture of TEOS and IBTS into the solution and, finally, slowly add the wetting agent into the solution, continue the reaction for 1 h after all components are added, and leave to cool until the tetraethyl orthosilicate surface treatment agent is obtained. In this paper, A, B, and C denote concrete specimens surface-treated with tetraethyl orthosilicate surface treatment agents with acrylic

acid, phosphoric acid, and hydrochloric acid as catalysts, respectively, while D denotes concrete specimens without surface treatment.

According to the different test contents, the surface treatment methods can be divided into two kinds: immersion, and surface impregnation. For anti-chlorine-ion-penetration testing using the immersion method, the test piece is immersed in a container with tetraethyl orthosilicate surface treatment agent to soak for 2 h; the liquid surface is higher than the top surface of the test piece (about 10 mm). In addition to the anti-chlorine-ion-penetration test, other tests use the surface impregnation method, e.g., the test face down with tetraethyl orthosilicate surface treatment agent surface impregnation treatment for 2 h, immersed in the liquid surface at a height of about 10 mm.

2.2. Methods

2.2.1. Water Absorption Tests

According to the JTJ 275-2000 technical specifications for corrosion prevention for concrete structures in marine harbor engineering [33], the tests were conducted using 100 mm × 100 mm × 100 mm cubic specimens. The specimens were put into the oven at 40 °C for 48 h after standard maintenance for 28 days, and the surface layer was impregnated for 2 h after drying and cooling, maintained in an indoor environment at $T = 20 \pm 2$ °C and $RH = 50 \pm 10\%$ for 7 days, and the surfaces were sealed with epoxy resin on the 5th day, except for the absorbent surface where the test was to be conducted. The sealed specimens were put into the oven at 40 °C again for 48 h and then weighed. A clear plastic box was used for the tests, and several 1 cm diameter glass rods were placed at the bottom of the box. The test specimen was placed on the glass rods with the absorbent surface facing downward, and water at 23 °C was slowly injected until the water surface reached a height of 1~2 mm on the glass rods. Then, the water absorption weight gain of the specimen was weighed at intervals of 5, 10, 30, 60, 120, and 140 min. Each group consisted of 3 specimens. The water absorption test chart is shown in Figure 2.



Figure 2. Water absorption test chart (D = not surfaced, A = surfaced with tetraethyl orthosilicate surface treatment agents with acrylic acid, B = surfaced with tetraethyl orthosilicate surface treatment agents with phosphoric acid, C = surfaced with tetraethyl orthosilicate surface treatment agents with hydrochloric acid).

The water absorption weight gain of each interval was converted into the water absorption height (mm); the water absorption height was taken as the vertical coordinate, the square root of the corresponding time interval was taken as the horizontal coordinate to draw the water absorption rate graph, and the slope of the line ($\text{mm}/\text{min}^{1/2}$) was taken as the average water absorption rate of the concrete specimen.

2.2.2. Water Contact Angle Tests

The tests were carried out using 100 mm × 100 mm × 100 mm cube specimens. After standard maintenance for 28 days, the specimens were put into the 40 °C oven to dry for

48 h, dried and cooled after the surface impregnation treatment for 2 h, and kept in an indoor environment at $T = 20 \pm 2 \text{ }^\circ\text{C}$ and $\text{RH} = 50 \pm 10\%$ for 7 days. Taking the small surface test water contact angle, we used distilled water for the test. Five points were randomly selected to test on the test surface, and the average value was taken as the test result, with an accuracy of 0.1° . A DSA100 contact angle measuring instrument (Krüss company, Hamburg, Germany), as shown in Figure 3, was used for the tests.

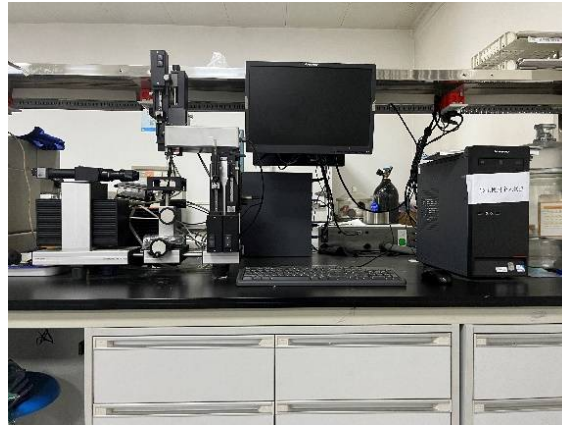


Figure 3. DSA100 contact angle measuring instrument.

2.2.3. Water Penetration Tests

Under the GB/T 50082-2009 standard for test methods for the long-term performance and durability of ordinary concrete [34], the water penetration height was tested using $\varnothing 175 \text{ mm} \times \varnothing 185 \text{ mm} \times 150 \text{ mm}$ specimens. The round table body specimens were maintained for 28 days and then dried to the lower bottom surface (i.e., the water-bearing pressure surface), followed by surface impregnation for 2 h in an indoor environment at $T = 20 \pm 2 \text{ }^\circ\text{C}$ and $\text{RH} = 50 \pm 10\%$ for 7 days after the start of the test. The tests started 24 h after splitting the specimen to measure the water penetration height, with 6 specimens in each group. The SRINK-50 intelligent automatic concrete impermeability instrument (Beijing Sona Checking and Controlling Technology Co., Ltd., Beijing, China), as shown in Figure 4, was used for the test.



Figure 4. SRINK-50 intelligent automatic concrete impermeability instrument.

2.2.4. Chloride Penetration Resistance Tests

The tests were performed according to the electric flux method described in the GB/T 50082-2009 standard for test methods of long-term performance and durability of ordinary concrete [34], using cured cylindrical specimens of $\varnothing 100 \text{ mm} \times 50 \text{ mm}$. The specimens were taken out and dried after 28 days. After drying and cooling, they were soaked in

the surface treatment agent for 2 h. They were maintained in an indoor environment at $T = 20 \pm 2 \text{ }^\circ\text{C}$ and $\text{RH} = 50 \pm 10\%$ for 8 days, and then placed in distilled water for 2 days to ensure that the concrete was in a water-absorbing saturated state. Then, the specimens were coated with epoxy resin on the side, and the vacuum saturation and electric flux tests were started after the epoxy resin was cured, with 3 specimens in each group. The SRH intelligent concrete vacuum saturation machine (Beijing Sona Checking and Controlling Technology Co., Ltd., Beijing, China), as shown in Figure 5, was used for the test.



Figure 5. SRH intelligent concrete vacuum saturation machine.

2.2.5. Carbonation Tests

The tests were conducted according to the carbonation test method described in the GB/T 50082-2009 standard for test methods of long-term performance and durability of ordinary concrete [34], using $100 \text{ mm} \times 100 \text{ mm} \times 400 \text{ mm}$ specimens. The prismatic specimen was put into the oven at $60 \text{ }^\circ\text{C}$ for 48 h after 28 days of maintenance, and the surface layer was impregnated for 2 h after drying and cooling. Then, the test was started after 7 days of maintenance in an indoor environment at $T = 20 \pm 2 \text{ }^\circ\text{C}$ and $\text{RH} = 50 \pm 10\%$. The test specimens were dried in the oven at $60 \text{ }^\circ\text{C}$ for 48 h, and then sealed with heated paraffin wax, except for one side that was left as the surface for measuring the carbonization depth. Then, parallel lines were drawn with a pencil along the length direction on the exposed side, with a 10 mm spacing, which was used as the measuring point. Each group consisted of 3 specimens. The CCB-70F concrete carbonation test chamber (Beijing Sona Checking and Controlling Technology Co., Ltd., Beijing, China), as shown in Figure 6, was used for the tests.



Figure 6. CCB-70F concrete carbonation test chamber.

When the specimen carbonation process was carried out for 3, 7, 14, and 28 days, the specimens were taken out and broken to determine the carbonation depth. The specimens

were broken through by the splitting method of the pressure testing machine, and the thickness of each excision was 80 mm. After cutting, the broken specimens were sealed with paraffin wax and put into the carbonation chamber to continue carbonation until the next test period.

Part of the brush was excised from the test piece to remove the residual powder on the section, and then sprayed with a concentration of 1% phenolphthalein alcohol solution (alcohol solution containing 20% steaming water). After about 30 s, the part of the concrete that was not carbonized became red. According to the original mark delineated with a Vernier caliper, a measurement point was delineated every 10 mm with a steel plate ruler to measure the depth of carbonation, and the arithmetic mean of each point was taken as the final depth of carbonation according to Formula (1):

$$\bar{d}_t = \frac{1}{n} \sum_{i=1}^n d_i \quad (1)$$

where \bar{d}_t is the average carbonization depth of the specimen after carbonization for t days (mm), accurate to 0.1 mm; d_i is the carbonization depth of each measurement point (mm); and n is the total number of measurement points.

2.2.6. SEM Tests

Scanning electron microscopy (SEM) tests were performed using a Quattro field-emission scanning electron microscope (Thermo Fisher Scientific Company, Waltham, MA, USA), as shown in Figure 7. The concrete samples were first dried for 24 h, and then gold-sprayed and scanned at the surface and 1 mm below the surface plane to determine the microscopic morphology. All photographs were taken at 10,000 \times magnification.

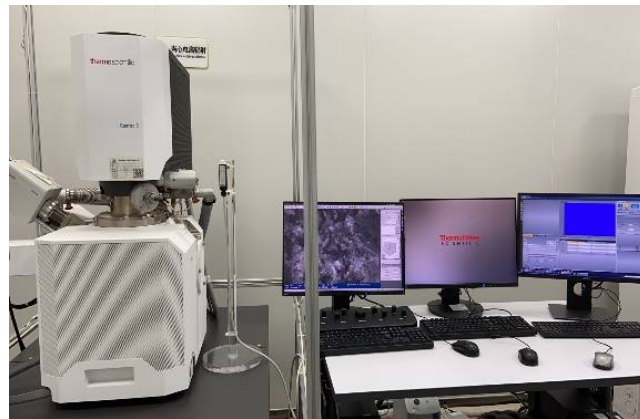


Figure 7. Quattro field-emission scanning electron microscope.

2.2.7. Pore Structure Analysis

The tests were conducted following the mercury intrusion porosimetry (MIP) method [35], and the pore structure characteristic parameters such as porosity and pore size distribution were tested after the concrete samples were dried for 24 h. The full-scan mode was used, the mercury contact angle was 130°, the mercury density was 13.53 g/mL, the mercury surface tension was 485 dynes/cm, and the pressure range was 0.1~60,000 psi. The AutoPore IV 9500 V1.09 fully automatic mercury piezometer (Micromeritics (Shanghai) Instrument Corporation, Shanghai, China), as shown in Figure 8, was used for the tests.



Figure 8. AutoPore IV 9500 V1.09 fully automatic mercury piezometer.

3. Results and Discussion

3.1. Water Absorption Test Results and Analysis

Table 2 shows the water absorption mass of concrete before and after surface treatment, and Figure 9 shows the relationship between the water absorption mass of concrete and time, before and after surface treatment.

Table 2. Water absorption mass of concrete before and after surface treatment (D = not surfaced, A = surfaced with tetraethyl orthosilicate surface treatment agents with acrylic acid, B = surfaced with tetraethyl orthosilicate surface treatment agents with phosphoric acid, C = surfaced with tetraethyl orthosilicate surface treatment agents with hydrochloric acid).

Sample	Water Absorption Mass at Different Times/g					
	5 min	15 min	45 min	105 min	225 min	365 min
D	2.43	3.27	4.33	5.50	6.73	7.40
A	0.20	0.33	0.50	0.73	0.93	1.00
B	0.33	0.57	0.70	0.90	1.10	1.27
C	0.13	0.27	0.47	0.60	0.80	0.93

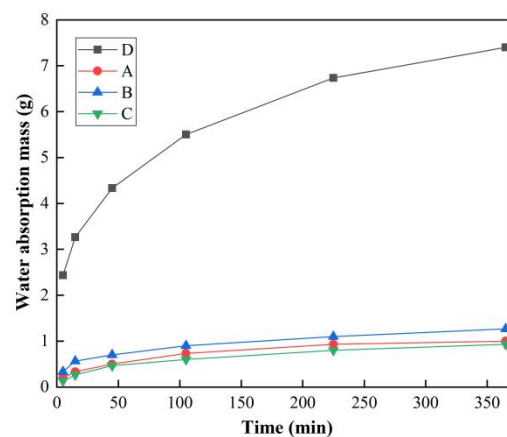


Figure 9. Relationship between the water absorption mass of concrete and time, before and after surface treatment (D = not surfaced, A = surfaced with tetraethyl orthosilicate surface treatment agents with acrylic acid, B = surfaced with tetraethyl orthosilicate surface treatment agents with phosphoric acid, C = surfaced with tetraethyl orthosilicate surface treatment agents with hydrochloric acid).

From Table 2 and Figure 9, it can be seen that the water absorption rate of concrete gradually slowed down with the extension of time. For the surface treatment group,

the increase in water absorption mass at 105 min leveled off, and the water absorption mass reached 73%, 70.9%, and 64.5% at 365 min, while the water absorption rate of the untreated group was still higher at 365 min. The trend of the water absorption rate of the surface treatment group slowing down with the extension of time was more obvious than that of the untreated group. The surface treatment agent tetraethyl orthosilicate had a significant weakening effect on the water absorption of concrete, and the final water absorption mass was only about 1 g. This was because after the surface treatment with the tetraethyl orthosilicate surface treatment agent, the concrete specimens were denser, and the generated hydrated calcium silicate gel filled the channels for external water to enter the concrete, significantly reducing the water absorption mass.

Table 3 shows the water absorption height and water absorption rate of concrete before and after surface treatment, while Figure 10 shows the relationship between water absorption height and the square root of the time interval of concrete before and after surface treatment.

Table 3. Water absorption height and water absorption rate of concrete before and after surface treatment (D = not surfaced, A = surfaced with tetraethyl orthosilicate surface treatment agents with acrylic acid, B = surfaced with tetraethyl orthosilicate surface treatment agents with phosphoric acid, C = surfaced with tetraethyl orthosilicate surface treatment agents with hydrochloric acid).

Sample	Water Absorption Height at the Corresponding Time Interval/mm						R ²	Water Absorption Rate/(mm/min ^{1/2})
	5 min	10 min	30 min	60 min	120 min	140 min		
D	0.243	0.327	0.433	0.550	0.673	0.740	0.993	0.04883
A	0.020	0.033	0.050	0.073	0.093	0.100	0.991	0.00811
B	0.033	0.057	0.070	0.090	0.110	0.127	0.972	0.00857
C	0.013	0.027	0.047	0.060	0.080	0.093	0.986	0.00766

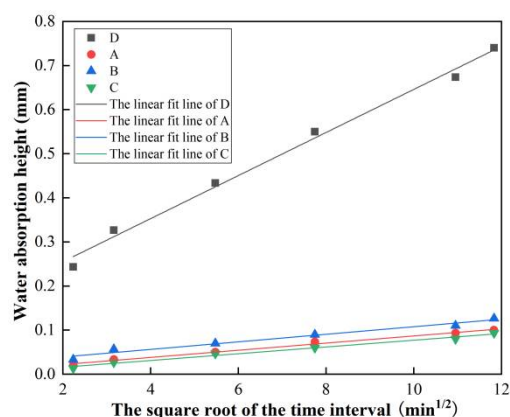


Figure 10. Relationship between water absorption height and the square root of the time interval of concrete, before and after surface treatment (D = not surfaced, A = surfaced with tetraethyl orthosilicate surface treatment agents with acrylic acid, B = surfaced with tetraethyl orthosilicate surface treatment agents with phosphoric acid, C = surfaced with tetraethyl orthosilicate surface treatment agents with hydrochloric acid).

From Table 3 and Figure 10, it can be seen that the water absorption height and the square root of the time interval were linearly fitted with R² greater than 0.97. All three tetraethyl orthosilicate surface treatment agents were able to significantly reduce the water absorption rate of concrete, and the average water absorption rates of concrete in the acrylic acid group, phosphoric acid group, and hydrochloric acid group were 0.00811, 0.00857, and 0.00766 mm/min^{1/2}, respectively, which were 83.4%, 82.4%, and 84.3% lower than those of the untreated group (0.04883 mm/min^{1/2}), respectively, with the best effect in the hydrochloric acid group, the second-best in the acrylic acid group, and a relatively poor effect in the phosphoric acid group, but the difference was no more than 0.0012 mm/min^{1/2}.

3.2. Water Contact Angle Test Results and Analysis

Figure 11 shows the water contact angle of the concrete before and after surface treatment.

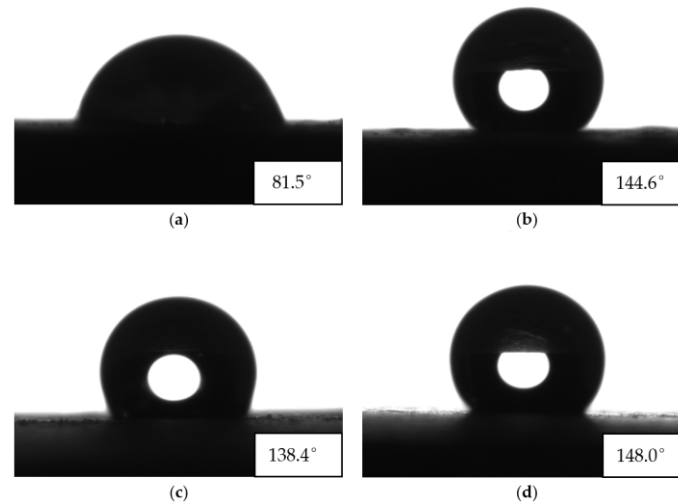


Figure 11. The water contact angle of concrete before and after surface treatment: (a) D, (b) A, (c) B, (d) C.

From Figure 11, it can be seen that the water contact angle of the concrete after surface treatment increased significantly. The concrete of the untreated group showed hydrophilicity (contact angle less than 90°), while the water contact angle of the concrete of the acrylic acid group, phosphoric acid group, and hydrochloric acid group reached 144.6° , 138.4° and 148.0° , respectively, showing a significant water-repellent effect. Among them, the water contact angle of the concrete in the hydrochloric acid group was the largest, followed by the acrylic acid group, while that of the phosphoric acid group was the smallest. This is consistent with the results of the water absorption tests, indicating that all three tetraethyl orthosilicate surface treatment agents were able to change the water contact angle of concrete from acute to obtuse, weakening the adsorption of water by capillaries and, thus, significantly improving the hydrophobic properties of concrete and strengthening its water repellency.

3.3. Water Penetration Test Results and Analysis

Figure 12 shows the water penetration height of the concrete before and after surface treatment, while Figure 13 shows the reduction rate of water penetration height after surface treatment.

From Figures 12 and 13, it can be seen that all three tetraethyl orthosilicate surface treatment agents effectively enhanced the water penetration resistance of concrete, with the acrylic acid group having the best effect, followed by the hydrochloric acid group, and the phosphoric acid group having a relatively poor effect. The water penetration heights of concrete in the acrylic acid group, phosphoric acid group, and hydrochloric acid group were 21, 28, and 23 mm, respectively, which were reduced by 63.2%, 50.9%, and 59.6%, respectively, compared to the untreated group (57 mm). This was because the tetraethyl orthosilicate surface treatment agent can react with calcium hydroxide to produce hydrated calcium silicate gel; the gel can plug the pores and fill the cracks, and forms a water-repellent layer on the concrete surface and in the capillaries to improve the water penetration resistance of the concrete.

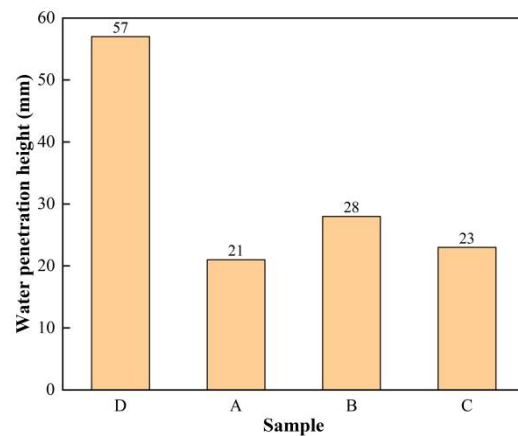


Figure 12. Water penetration height of the concrete before and after surface treatment (D = not surfaced, A = surfaced with tetraethyl orthosilicate surface treatment agents with acrylic acid, B = surfaced with tetraethyl orthosilicate surface treatment agents with phosphoric acid, C = surfaced with tetraethyl orthosilicate surface treatment agents with hydrochloric acid).

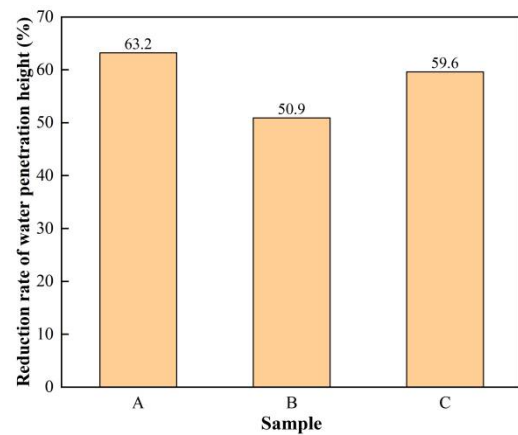


Figure 13. Reduction rate of water penetration height after surface treatment (A = surfaced with tetraethyl orthosilicate surface treatment agents with acrylic acid, B = surfaced with tetraethyl orthosilicate surface treatment agents with phosphoric acid, C = surfaced with tetraethyl orthosilicate surface treatment agents with hydrochloric acid).

3.4. Rapid Chloride Penetration Test (RCPT) Results and Analysis

Table 4 shows the relationship between the electrical flux of concrete and chloride ion penetration [36]. Figure 14 shows the chloride ion flux of the concrete before and after surface treatment, while Figure 15 shows the reduction rate of the electric flux of concrete after the surface treatment.

Table 4. Chloride ion penetrability based on charge passed.

Charge Passed/C	>4000	2000–4000	1000–2000	100–1000	<100
Chloride Ion Penetrability	High	Moderate	Low	Very Low	Negligible

As can be seen from Figures 14 and 15, all three tetraethyl orthosilicate surface treatment agents effectively reduced the chloride ion permeability of concrete, and the chloride ion permeability level of the concrete after the surface treatments was reduced from medium to very low. Among them, the hydrochloric acid group had the best effect, followed by the acrylic acid group, while the phosphoric acid group was relatively poor. The chloride ion fluxes of concrete in the acrylic acid, phosphoric acid, and hydrochloric acid groups were

567C, 671C, and 462C, respectively, which were 74%, 69.2%, and 78.8% lower than those in the untreated group (2180C), respectively. This was because the tetraethyl orthosilicate surface treatment agent penetrates the concrete and reacts with the concrete hydration products to generate gels that plug pores and microcracks, while the reduction in water absorption of concrete also reduces the chloride ion migration, thus reducing the chloride ion permeability of concrete.

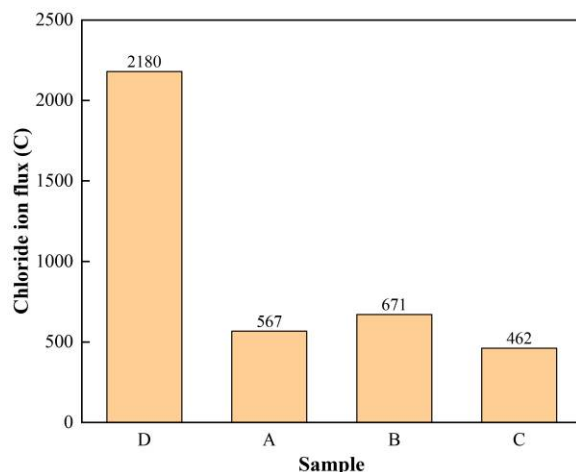


Figure 14. Chloride ion flux of the concrete before and after surface treatment (D = not surfaced, A = surfaced with tetraethyl orthosilicate surface treatment agents with acrylic acid, B = surfaced with tetraethyl orthosilicate surface treatment agents with phosphoric acid, C = surfaced with tetraethyl orthosilicate surface treatment agents with hydrochloric acid).

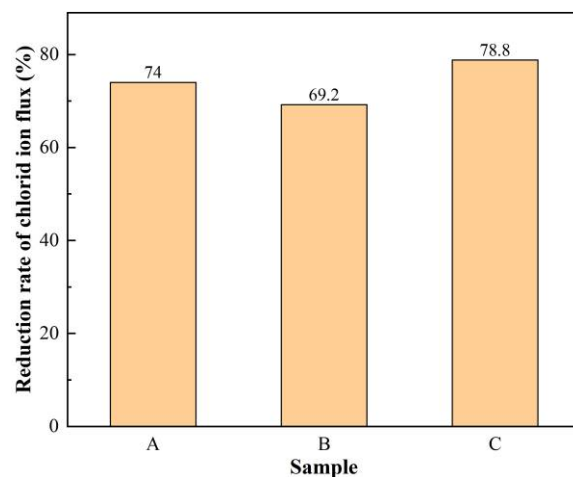


Figure 15. Reduction rate of chloride ion flux of concrete after the surface treatment (A = surfaced with tetraethyl orthosilicate surface treatment agents with acrylic acid, B = surfaced with tetraethyl orthosilicate surface treatment agents with phosphoric acid, C = surfaced with tetraethyl orthosilicate surface treatment agents with hydrochloric acid).

3.5. Carbonation Test Results and Analysis

Table 5 shows the carbonation depth of concrete before and after surface treatment, while Figure 16 shows the curves of the carbonation depth of concrete before and after surface treatment with the age of carbonation.

From Table 5, it can be seen that all three tetraethyl orthosilicate surface treatment agents significantly reduced the carbonation depth of concrete. The phosphoric acid group had the most obvious effect, with a carbonation depth of 1.0 mm in 28 days, which was 87.2% lower than that of the untreated group. The hydrochloric acid group had the second-highest effect, with a carbonation depth of 2.4 mm in 28 days, which was 69.2% lower than

that of the untreated group. The acrylic acid group had a relatively poor effect, with a carbonation depth of 3.2 mm in 28 days, which was 59.0% lower than that of the untreated group. The main reason was that the three tetraethyl orthosilicate surface treatment agents can react with cement hydration products to produce a gel, which improves the compactness of the concrete surface and reduces the entry of carbon dioxide, while the phosphoric-acid-catalyzed tetraethyl orthosilicate surface treatment agent forms a film on the concrete surface. Although the film had little effect on the waterproofing effect, the effect of gas protection was more obvious, so the carbonation resistance of the phosphoric acid group showed the most significant performance improvement.

From Figure 16, it can be seen that with the increase in carbonation age, the growth trend of concrete carbonation depth in the surface-treated group gradually slowed down. While the growth trend of carbonation depth in the untreated group also slowed down gradually, the growth rate was still relatively high compared to the surface-treated groups. This was because the gel generated by the reaction between the tetraethyl orthosilicate surface treatment agents and the concrete improved the compactness of the concrete surface, increased the difficulty of carbon dioxide entering the concrete, reduced the amount of carbon dioxide entering the concrete, and decreased the growth rate of the carbonation depth. The denseness of the concrete surface in the untreated group was much lower than that in the surface-treated groups, so the growth rate of the carbonation depth was greater than that in the surface-treated groups.

Table 5. Water absorption mass of concrete before and after surface treatment (D = not surfaced, A = surfaced with tetraethyl orthosilicate surface treatment agents with acrylic acid, B = surfaced with tetraethyl orthosilicate surface treatment agents with phosphoric acid, C = surfaced with tetraethyl orthosilicate surface treatment agents with hydrochloric acid).

Sample	Carbonation Depth at Different Carbonation Ages/mm			
	3 days	7 days	14 days	28 days
D	1.5	3.1	4.8	7.8
A	0.5	1.7	2.6	3.2
B	0.1	0.5	0.8	1.0
C	0.3	1.2	1.9	2.4

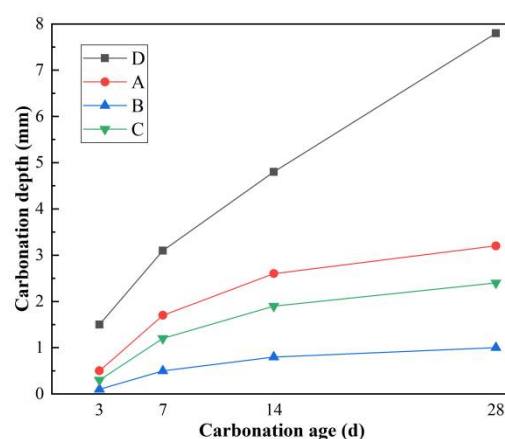


Figure 16. Curves of the carbonation depth of concrete before and after surface treatment with the age of carbonation (D = not surfaced, A = surfaced with tetraethyl orthosilicate surface treatment agents with acrylic acid, B = surfaced with tetraethyl orthosilicate surface treatment agents with phosphoric acid, C = surfaced with tetraethyl orthosilicate surface treatment agents with hydrochloric acid).

3.6. SEM Test Results and Analysis

Figure 17 shows the microscopic morphology of concrete before and after surface treatment.

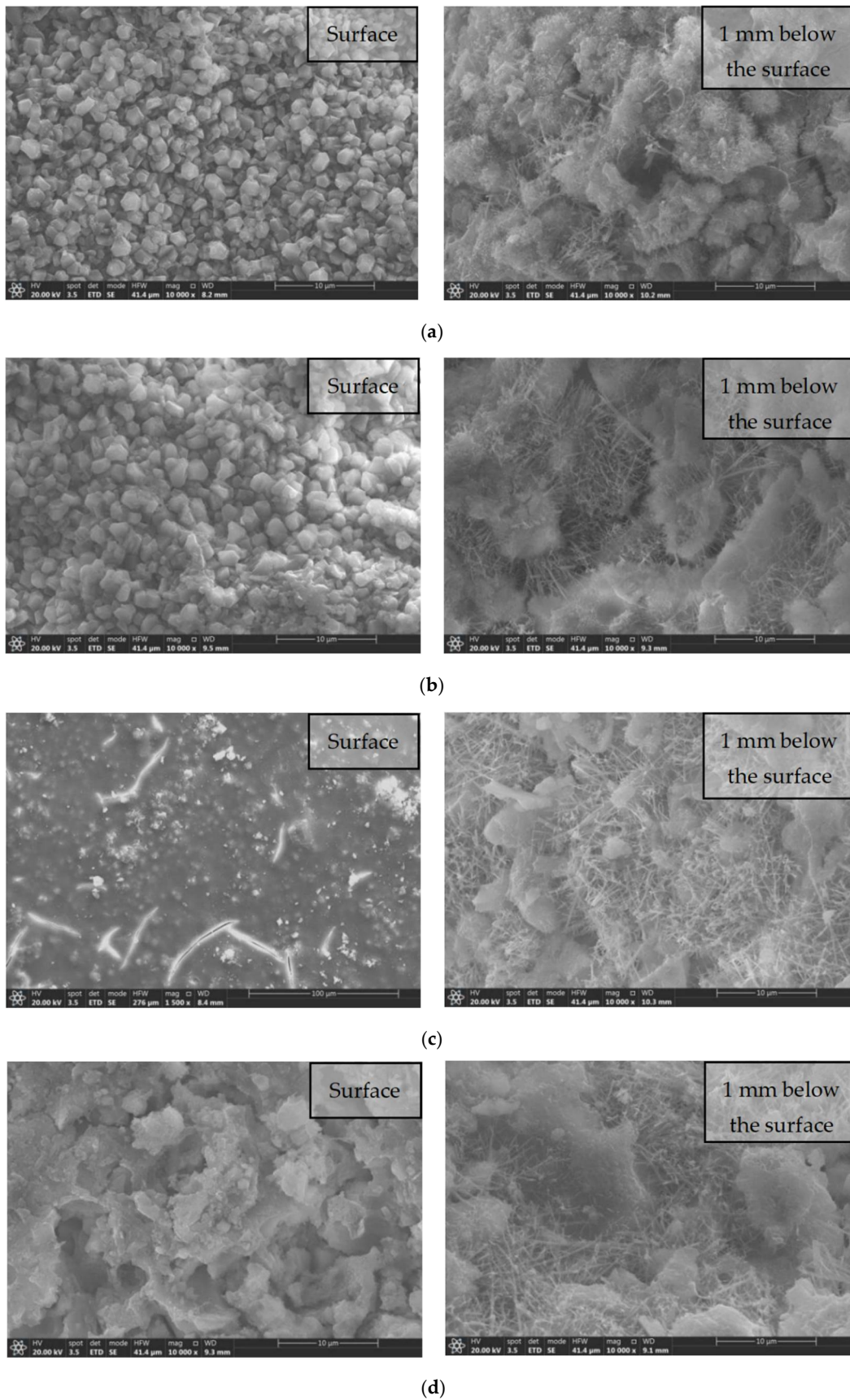


Figure 17. Microscopic morphology of concrete before and after surface treatment: (a) D (b) A (c) B (d) C.

From Figure 17a, it can be seen that the surface of the concrete in the untreated group is mainly hexagonal plate-like calcium hydroxide crystals and a small amount of granular hydrated calcium silicate, with microcracks and pores visible. At 1 mm below the surface, the main component is clustered hydrated calcium silicate, and the hydrated calcium silicate is interspersed with needle and rod structures on the surface, while laminated calcium hydroxide crystals and coarse pores are still present. As can be seen in Figure 17b, the microcracks and pores on the concrete surface of the acrylic acid group are significantly reduced, and the surface is denser, with hexagonal plate-like calcium hydroxide crystals and laminated calcium hydrosilicate roughly accounting for half each. At 1 mm below the surface, the main component is lamellar hydrated calcium silicate, and the rest of the space consists of needle- and rod-like structures, with almost no calcium hydroxide crystals visible. As can be seen in Figure 17c, a film is formed on the surface of the phosphoric acid group concrete, but there are microcracks in the film, which may be the reason why the phosphate-catalyzed tetraethyl orthosilicate surface treatment can significantly reduce the depth of concrete carbonation, but has no significant effect on other properties. At 1 mm below the surface, the lamellar structure of hydrated calcium silicate becomes weaker as a whole; the needle-rod structure occupies the main part, and a small amount of plate-like calcium hydroxide crystals can still be found. From Figure 17d, it can be seen that the surface of the concrete in the hydrochloric acid group is mainly tightly bound slab-like hydrated calcium silicate, while there are calcium hydroxide crystals on the surface of the hydrated calcium silicate, but there are large pores in the surface layer, which may be caused by the uneven impregnation of the surface layer of the tetraethyl orthosilicate surface treatment agent. At 1 mm below the surface, the lamellar structure of the hydrated calcium silicate is tight, the needle and rod structures are significantly reduced, and no calcium hydroxide crystals are present.

In summary, it can be seen that (1) compared with the untreated group, the microcracks and pores of the concrete in the surface treatment group were significantly reduced or even disappeared, and the surface treatment improved the compactness of the concrete surface; (2) the number of calcium hydroxide crystals of the concrete in the surface treatment group was significantly reduced, indicating that a secondary hydration reaction occurred between the tetraethyl orthosilicate surface treatment agent and the concrete, which consumed calcium hydroxide; (3) the amount of hydrated calcium silicate in the surface treatment groups was significantly increased, and the hydrated calcium silicate in the untreated group was mainly in clusters, while that in the surface treatment groups was mainly in sheets and plates, with a more compact structure; and (4) the phosphoric-acid-catalyzed tetraethyl orthosilicate surface treatment agent formed a film on the surface of the concrete, but the strength and the denseness of the film were not very high, providing a certain protective effect against gas, but no protection against water and ion penetration.

3.7. Pore Structure Analysis Results and Analysis

Table 6 shows the characteristic parameters of the pore structure of concrete before and after surface treatment, while Figure 18 shows the pore size distribution of concrete before and after surface treatment.

As seen in Table 6, the most common pore sizes of the specimens in each group were almost unchanged, indicating that the surface treatment did not change the most common pore sizes of the concrete. As can be seen from Figure 18, the surface treatment reduced the porosity of the concrete, which was 25.35% in the untreated group and 14.17%, 18.26%, and 15.36% in the acrylic acid, phosphoric acid, and hydrochloric acid groups, respectively, which were 44.10%, 27.97%, and 39.40% lower compared to the untreated group, respectively. Meanwhile, the surface treatment reduced the proportion of harmful pores (100~1000 nm) and multi-harmful pores (>1000 nm) in the concrete, and increased the proportion of harmless pores (<10 nm) and less harmful pores (10~100 nm), among which the proportion of less harmful pores (10~100 nm) and harmful pores (100~1000 nm) was the largest, compared with the untreated group, the acrylic acid group, the hydrochloric

acid group, and the phosphoric acid group. Compared with the untreated group, the proportions of harmful pores (100~1000 nm) in the acrylic acid, hydrochloric acid, and phosphoric acid groups decreased by 58.89%, 37.55%, and 47.04%, respectively, and the proportions of less harmful pores (10~100 nm) increased by 27.98%, 16.39%, and 23.18%, respectively. These results show that the tetraethyl orthosilicate surface treatment agent can plug concrete pores, refine the pore size, improve the pore structure, and reduce the total porosity and the number of multi-harmful and harmful pores of the concrete, explaining its ability to reduce the water absorption of concrete and improve its water permeability.

Table 6. Characteristic parameters of pore structure of concrete before and after surface treatment (D = not surfaced, A = surfaced with tetraethyl orthosilicate surface treatment agents with acrylic acid, B = surfaced with tetraethyl orthosilicate surface treatment agents with phosphoric acid, C = surfaced with tetraethyl orthosilicate surface treatment agents with hydrochloric acid).

Sample	Porosity/%	The Most Available Aperture/nm	Aperture Ratio/%			
			<10 nm	10~100 nm	100~1000 nm	>1000 nm
D	25.35	62.54	2.8	60.4	25.3	11.4
A	14.17	62.56	5.7	77.3	10.4	6.6
B	18.26	62.57	4.5	70.3	15.8	9.4
C	15.36	62.53	5.1	74.4	13.4	7.1

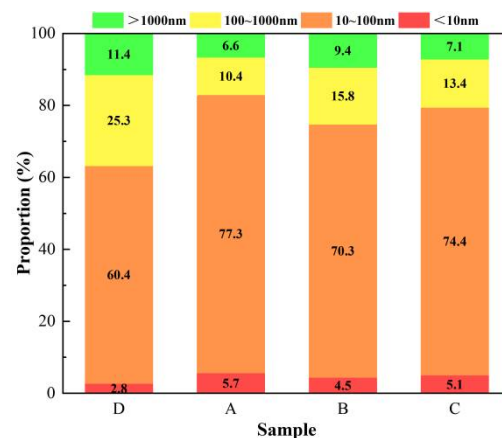


Figure 18. Pore size distribution of concrete before and after surface treatment (D = not surfaced, A = surfaced with tetraethyl orthosilicate surface treatment agents with acrylic acid, B = surfaced with tetraethyl orthosilicate surface treatment agents with phosphoric acid, C = surfaced with tetraethyl orthosilicate surface treatment agents with hydrochloric acid).

4. Conclusions

In this paper, three modified tetraethyl orthosilicate surface treatment agents were prepared by hybridization and catalysis, and their effects on the impermeability of airport pavement surface concrete, along with their mechanisms of action, were studied through a series of tests. The following conclusions can be drawn:

- (1) The modified tetraethyl orthosilicate surface treatment agent with hydrochloric acid as a catalyst had the most obvious effect on the improvement of the impermeability of concrete, and this surface-treated concrete had the lowest water absorption, the largest water contact angle, and the best resistance to chloride ion penetration.
- (2) The overall enhancement effect of the modified tetraethyl orthosilicate surface treatment agent with acrylic acid as a catalyst on the impermeability of concrete was weaker than that of the modified tetraethyl orthosilicate surface treatment agent with hydrochloric acid as a catalyst, and was only slightly stronger than that of the modified tetraethyl orthosilicate surface treatment agent with hydrochloric acid as

a catalyst in terms of the improvement of water permeability, where the difference between them was not significant.

- (3) The modified tetraethyl orthosilicate surface treatment agent with phosphoric acid as a catalyst showed the most outstanding performance in the improvement of carbonation resistance, and the carbonation depth of concrete was only about 1 mm in 28 days, but the other performance indices were weaker than those of the other two surface treatment agents.
- (4) SEM and MIP tests showed that the modified tetraethyl orthosilicate surface treatment agents improved the impermeability of concrete mainly by blocking microcracks and pores with the resulting hydrated calcium silicate gel, reducing the total porosity of the concrete and the numbers of multi-harmful and harmful pores, and improving the compactness of the concrete.

In summary, all three tetraethyl orthosilicate surface treatment agents prepared in this paper can significantly enhance the impermeability of airport pavement surface concrete, and the results of this study can help the development of modified tetraethyl orthosilicate surface treatment agents and their application in airport pavement surface projects, as well as providing certain methods and ideas for the modification of concrete surface treatment agents.

Author Contributions: Conceptualization, T.L. and Y.W.; methodology, T.L.; software, T.L.; validation, Y.W.; formal analysis, T.L.; investigation, Y.W.; resources, T.L.; data curation, T.L.; writing—original draft preparation, T.L.; writing—review and editing, T.L.; visualization, T.L.; project administration, Y.W. All authors have read and agreed to the published version of the manuscript.

Funding: This research was funded by the National Natural Science Foundation of China, Grant No. 51608526.

Institutional Review Board Statement: Not applicable.

Informed Consent Statement: Not applicable.

Data Availability Statement: Not applicable.

Acknowledgments: The authors express thanks to all members of the laboratory team for their help with the technical support.

Conflicts of Interest: The authors declare no conflict of interest.

References

1. Chen, Y.; Cen, G.; Cui, Y. Comparative analysis on the anti-wheel impact performance of steel fiber and reticular polypropylene synthetic fiber reinforced airport pavement concrete under elevated temperature aging environment. *Constr. Build. Mater.* **2018**, *192*, 818–835. [[CrossRef](#)]
2. Guo, T.; Weng, X. Evaluation of the freeze-thaw durability of surface-treated airport pavement concrete under adverse conditions. *Constr. Build. Mater.* **2019**, *206*, 519–530. [[CrossRef](#)]
3. Cheng, X.; Shah, S.P.; Cao, W.; Qian, J.; Hou, P. Characteristics of surface-treatment of nano-SiO₂ on the transport properties of hardened cement pastes with different water-to-cement ratios. *Cem. Concr. Compos.* **2015**, *55*, 26–33.
4. Ali, S.; Fawzia, S.; Thambiratnam, D.; Liu, X.; Remennikov, A.M. Performance of protective concrete runway pavement under aircraft impact loading. *Struct. Infrastruct. Eng.* **2020**, *12*, 1698–1710. [[CrossRef](#)]
5. Hui, M.; Zz, A. Paving an engineered cementitious composite (ECC) overlay on concrete airfield pavement for reflective cracking resistance. *Constr. Build. Mater.* **2020**, *252*, 119048.
6. Han, Y.M.; Dong, G.S.; Choi, D.S. Evaluation of the durability of mortar and concrete applied with inorganic coating material and surface treatment system. *Constr. Build. Mater.* **2007**, *21*, 362–369.
7. Tfaa, C.; Aoad, E.; Dooab, C.; Ooa, F.; Boo, G. Effects of calcined clay, sawdust ash and chemical admixtures on Strength and properties of concrete for pavement and flooring applications using Taguchi approach—ScienceDirect. *Case Stud. Constr. Mater.* **2021**, *15*, e00568.
8. Lai, Y.; Liu, Y.; Wang, P.; Ma, D.X.; Hou, S. Effect of aircraft deicer on deicer-scaling resistance and frost resistance of airport pavement concrete. *J. Phys. Conf. Ser.* **2020**, *1605*, 012178. [[CrossRef](#)]
9. Yang, G.Q.; Sun, Z.J. Experimental study about the influence of silane impregnation on the durability of airport pavement concrete in aircraft deicing fluid environment. *IOP Conf. Ser. Earth Environ. Sci.* **2021**, *787*, 012007. [[CrossRef](#)]

10. Bertolini, L.; Elsener, B.; Pedferri, P.; Polder, R. *Corrosion of Steel in Concrete: Prevention, Diagnosis, Repair*; Wiley-VCH Verlag GmbH & Co. KGaA: Hoboken, NJ, USA, 2013; Volume 49, pp. 4113–4133.
11. Mundo, R.D.; Labianca, C.; Carbone, G.; Notarnicola, M. Recent advances in hydrophobic and icephobic surface treatments of concrete. *Coatings* **2020**, *10*, 449. [[CrossRef](#)]
12. Mehta, P.K. Durability of concrete—fifty years of progress. *Spec. Publ.* **1991**, *1*, 1–31.
13. Coffetti, D.; Crotti, E.; Gazzaniga, G.; Gottardo, R.; Pastore, T.; Coppola, L. Protection of concrete structures: Performance analysis of different commercial products and systems. *Materials* **2021**, *14*, 3719. [[CrossRef](#)]
14. Pan, X.; Shi, Z.; Shi, C.; Ling, T.C.; Ning, L. A review on surface treatment for concrete—Part 2: Performance. *Constr. Build. Mater.* **2017**, *133*, 81–90. [[CrossRef](#)]
15. Scarfato, P.; Maio, L.D.; Fariello, M.L.; Russo, P.; Incarnato, L. Preparation and evaluation of polymer/clay nanocomposite surface treatments for concrete durability enhancement. *Cem. Concr. Compos.* **2012**, *34*, 297–305. [[CrossRef](#)]
16. Liu, B.; Qin, J.; Sun, M. Influence of silane-based impregnation agent on the permeability of concretes. *KSCE J. Civil Eng.* **2019**, *23*, 3443–3450. [[CrossRef](#)]
17. Sojobi, A.O.; Xuan, D.; Li, L.; Liu, S.; Chi, S.P. Optimization of gas-solid carbonation conditions of recycled aggregates using a linear weighted sum method. *Dev. Built Environ.* **2021**, *7*, 100053. [[CrossRef](#)]
18. Pigino, B.; Leemann, A.; Franzoni, E.; Lura, P. Ethyl silicate for surface treatment of concrete—Part II: Characteristics and performance. *Cem. Concr. Compos.* **2011**, *34*, 313–321. [[CrossRef](#)]
19. Franzoni, E.; Pigino, B.; Pistolesi, C. Ethyl silicate for surface protection of concrete: Performance in comparison with other inorganic surface treatments. *Cem. Concr. Compos.* **2013**, *44*, 69–76. [[CrossRef](#)]
20. García-Vera, V.E.; Tenza-Abril, J.A.; Lanzón, M. The effectiveness of ethyl silicate as consolidating and protective coating to extend the durability of earthen plasters. *Constr. Build. Mater.* **2020**, *236*, 117445. [[CrossRef](#)]
21. Franzoni, E.; Pigino, B.; Leemann, A.; Lura, P. Use of TEOS for fired-clay bricks consolidation. *Mater. Struct.* **2014**, *47*, 1175–1184. [[CrossRef](#)]
22. Cai, Y.; Hou, P.; Duan, C.; Zhang, R.; Zhou, Z.; Cheng, X.; Shah, S. The use of tetraethyl orthosilicate silane (TEOS) for surface-treatment of hardened cement-based materials: A comparison study with normal treatment agents. *Constr. Build. Mater.* **2016**, *117*, 144–151. [[CrossRef](#)]
23. Barberena-Fernandez, A.M.; Blanco-Varela, M.T.; Carmona-Quiroga, P.M. Interaction of TEOS with cementitious materials: Chemical and physical effects. *Cem. Concr. Compos.* **2015**, *55*, 145–152. [[CrossRef](#)]
24. Chen, X.; Geng, Y.; Li, S.; Hou, D.; Ai, H. Preparation of modified silane composite emulsion and its effect on surface properties of cement-based materials. *Coatings* **2021**, *11*, 272. [[CrossRef](#)]
25. Franzoni, E.; Graziani, G.; Sassoni, E. TEOS-based treatments for stone consolidation: Acceleration of hydrolysis-condensation reactions by poulticing. *J. Sol-Gel Sci. Technol.* **2015**, *74*, 398–405. [[CrossRef](#)]
26. Sassoni, E.; Franzoni, E.; Pigino, B.; Scherer, G.W.; Naidu, S. Consolidation of calcareous and siliceous sandstones by hydroxyapatite: Comparison with a TEOS-based consolidant. *J. Cult. Herit.* **2013**, *14*, e103–e108. [[CrossRef](#)]
27. Miliani, C.; Velo-Simpson, M.L.; Scherer, G.W. Particle-modified consolidants: A study on the effect of particles on sol-gel properties and consolidation effectiveness. *J. Cult. Herit.* **2007**, *8*, 1–6. [[CrossRef](#)]
28. Sena, D.; Picarra, S.; Pinto, A.F.; Ferreira, M.J.; Montemor, M.F. TEOS-based consolidants for carbonate stones: The role of N1-(3-trimethoxysilylpropyl)diethylenetriamine. *New J. Chem.* **2017**, *41*, 2458–2467. [[CrossRef](#)]
29. Bracci, S.; Sacchi, B.; Pinto, A.; Rodrigues, J.D. Inorganic consolidants on stone artefacts: Optimisation of application procedures for marble and limestones. In Proceedings of the International Symposium “Stone Consolidation in Cultural Heritage Research and Practice”, Lisbon, Portugal, 6–7 May 2008; pp. 81–90.
30. Kim, E.K.; Won, J.; Do, J.Y.; Kim, S.D.; Yong, S.K. Effects of silica nanoparticle and GPTMS addition on TEOS-based stone consolidants. *J. Cult. Herit.* **2009**, *10*, 214–221. [[CrossRef](#)]
31. Chen, X.; Shao-Chun, L.I.; Gang, X.U.; Jin, Z.Q. Influence of the capillary water absorption and anti carbonization to concrete by TEOS-isobutyl silane compound emulsion. *Bull. Chin. Ceram. Soc.* **2016**, *9*, 7–13.
32. Zárrega, R.; Cervantes, J.; Salazar-Hernandez, C.; Wheeler, G. Effect of the addition of hydroxyl-terminated polydimethylsiloxane to TEOS-based stone consolidants. *J. Cult. Herit.* **2010**, *11*, 138–144. [[CrossRef](#)]
33. *JTJ 275-2000*; Corrosion Prevention Technical Specifications for Concrete Structures of Marine Harbour Engineering. China Architecture & Building Press: Beijing, China, 2001.
34. *GB/T 50082-2009*; Standard for Test Methods of Long-Term Performance and Durability of Ordinary Concrete. China Architecture & Building Press: Beijing, China, 2009.
35. *GB/T 21650.1-2008*; Pore Size Distribution and Porosity of Solid Materials by Mercury Porosimetry and Gas Adsorption—Part 1: Mercury Porometry. China Architecture & Building Press: Beijing, China, 2008.
36. *ASTM C1202-22*; Standard Test Method for Electrical Indication of Concrete’s Ability to Resist Chloride Ion Penetration. ASTM International: West Conshohocken, PA, USA, 1997; Volume 4, pp. 639–644.